



Synthesis, biological evaluation, and molecular docking of dihydroflavonol derivatives as anti-inflammatory agents

Yuanhang Xiang¹ · Chunling Hu¹ · Yuejie Zhang¹ · Xiaochuan Ye¹

Received: 28 November 2018 / Accepted: 29 March 2019
© Springer Science+Business Media, LLC, part of Springer Nature 2019

Abstract

A series of dihydroflavonol derivatives (**4a–4l**) were synthesized from chalcones via classical Algar–Flynn–Oyamada (AFO) reaction and characterized on the basis of spectroscopic analyses. All synthesized compounds were evaluated for their inhibitory activity against the pro-inflammatory-inducible TNF-alpha, IL-1beta, and IL-6 in lipopolysaccharide (LPS)-stimulated RAW 264.7 cell lines and showed various efficiency. Furthermore, compounds **4d** and **4k** were selected to examine their in vivo anti-inflammatory activity by using two classical models. Herein compound **4k** showed maximum anti-inflammatory activity of 32.98% inhibition in mice ear-swelling model and 40.06% inhibition at the 2 h intervals in rat paw edema model in comparison to the two references: aspirin and meloxicam. Similar effect was observed at a lower dose. In addition, the compound **4k** was docked against cyclooxygenases-2 to validate the attained pharmacological data and provide understandable evidence for the observed anti-inflammatory activity.

Keywords Inflammation · Dihydroflavonol · Molecular docking · Cytokine

Introduction

Inflammation is a condition of body immunity associated with damaged tissue or organ. The scientific community has always been interested in the treatment of inflammation (Cooke and Ferrari 2018). Many trials have been undertaken to identify compounds from natural resources that suppress or mitigate the progress of inflammation, especially in herbal medicine. Flavonoids are often designated as active constituents in many traditional medicinal plants (Devi et al. 2015).

Nowadays, naturally-occurring flavonoids are emerging as a vibrant chemical backbone that could help in the fight against several human diseases (Singh et al. 2014). Among which, dihydroflavonols have received more and more attention for novel structure and excellent pharmacological activities and been reported to have anti-allergic, anti-inflammation (Ayoub et al. 2018), anti-microbial (Karim

et al. 2016), anti-plasmodial (Muiva-Mutisya et al. 2018), and anti-proliferative (Sun et al. 2018) activities. Of which, the anti-inflammatory activity is one of the most important and versatile functions of dihydroflavonols (Ding et al. 2018; Sun et al. 2014; Topal et al. 2016)

In previous studies, we found a simple and effective synthetic route of dihydroflavonols by optimizing the reaction conditions (Hu et al. 2018). Herein, we synthesized a series of dihydroflavonol derivatives with 3,5,7-trihydroxy-2-phenylchroman-4-one skeleton by introducing different groups in the B ring as described in Scheme 1 and evaluated their anti-inflammatory activities in vitro and in vivo. In order to get insights into the binding modes of these molecules with hypothetical protein target, Autodock Vina was performed to dock the compounds into the active site of COX-2 (PDB:4M11). The anti-inflammatory effect of dihydroflavonol derivatives was duly supported by molecular docking studies.

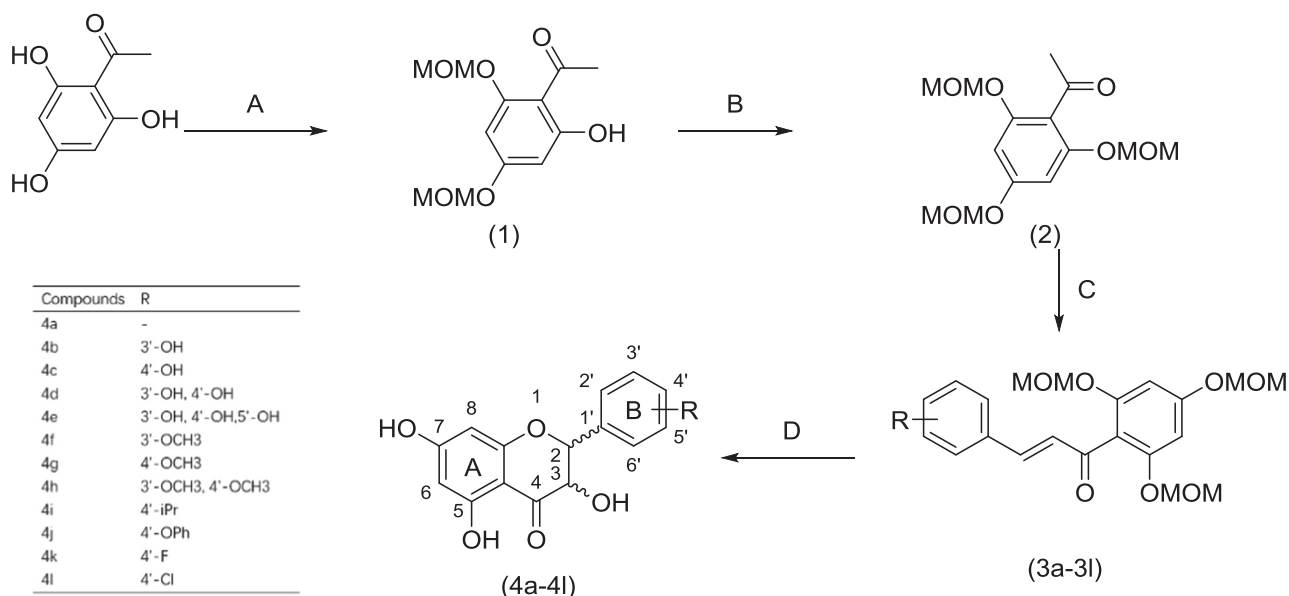
Materials and methods

Chemistry

All chemicals used for the synthesis of compounds were purchased from Sinopharm Chemical Reagent Co. Ltd.

✉ Chunling Hu
huchunling2007@hbtcu.edu.cn

¹ Key Laboratory of Chinese Medicine Chemistry and Chinese Herbal Compound of Hubei Province, Hubei University of Traditional Chinese Medicine, Wuhan 430065, China



Scheme 1 Synthesis of dihydroflavonol derivatives. Reagents and conditions. **a** DIPEA, MOMCl, CH₂Cl₂, 0 °C; **b** NaH, MOMCl, THF, 0 °C; **c** substituted benzaldehydes, NaOH, r.t.; **d** H₂O₂, NaOH, MeOH, then HCl, 55 °C

(China). All synthesized compounds were checked by thin layer chromatography (TLC) performed on Silica gel 60 GF₂₅₄ coated plates. The FT-IR spectra were recorded with Shimadzu FTIR-8400S spectrometer (Tokyo, Japan). Nuclear magnetic resonance (NMR) spectra were processed in DMSO-d₆ on a Bruker NMR spectrophotometer operating at 400 MHz for ¹H and 100 MHz for ¹³C. Mass spectrometer was used for the measurement of molecular masses of compounds.

General synthesis of dihydroflavonol derivatives (4a–4l)

MOM-protected chalcone derivatives (1.0 mmol) and aqueous NaOH solution (5 M, 10 ml) were added to methanol (15.0 ml). To the above reaction mixture, 30% H₂O₂ (0.3 ml, 3.0 mmol) was added and stirred for 3 h at room temperature. After completion of the reaction (as indicated by TLC), the reaction was quenched by saturated sodium sulfite and extracted with EtOAc. Then the epoxide was dissolved in methanol solution and treated with HCl at 55 °C. The crude material was purified via silica gel flash chromatography to give corresponding dihydroflavonol derivatives (4a–4l).

(E)-3-(3,4-bis(methoxymethoxy)phenyl)-1-(2,4,6-tris(methoxymethoxy)phenyl)-prop-2-en-1-one (3d)

Light yellow solid; yield: 78%; mp 131–132 °C; IR (KBr) ν_{\max} 2956, 2918, 1649, 1603, 1509, 1434, 1395, 1259, 1152, 1048, 922, 822, 755 cm⁻¹; ¹H NMR (DMSO-d₆, 400

MHz) δ 7.44 (1H, s, H-6), 7.29 (1H, d, $J = 8.5$ Hz, H-7), 7.18 (1H, d, $J = 16.0$ Hz, H-8), 7.11 (1H, d, $J = 8.4$ Hz, H-6), 6.91 (1H, d, $J = 16.1$ Hz, H-5), 6.52 (2H, s, H-3',5'), 5.24 (4H, s, 2',6'-OCH₂O-), 5.21 (2H, s, 4'-OCH₂O-), 5.14 (4H, s, 3,4-OCH₂O-), 3.41 (3H, s, 4'-OCH₃), 3.39 (6H, d, $J = 2.6$ Hz, 3,4-OCH₃), 3.27 (6H, d, $J = 1.0$ Hz, 2',6'-OCH₃); ¹³C NMR (DMSO-d₆, 100 MHz) δ 193.20 (C=O), 158.74 (C, C-4'), 154.99 (C, C-2',6'), 149.17 (C, C-3), 146.75 (C, C-4), 144.51 (CH, C-8), 128.30 (C, C-1), 127.51 (CH, C-7), 123.82 (CH, C-6), 116.42 (CH, C-5), 116.17 (CH, C-2), 114.41 (C, C-1'), 96.55 (CH, C-3',5'), 94.63 (CH₂, 4-OCH₂O-), 94.41 (CH₂, 3-OCH₂O-), 94.12 (CH₂, 4'-OCH₂O-), 93.90 (CH₂, 2',6'-OCH₂O-), 55.96 (CH₃, 4-OCH₃), 55.85 (CH₃, 3-OCH₃), 55.83 (CH₃, 4'-OCH₃), 55.76 (CH₃, 2',6'-OCH₃); EIMS m/z : 508.0 [M]⁺.

(E)-3-(4-fluorophenyl)-1-(2,4,6-tris(methoxymethoxy)phenyl)prop-2-en-1-one (3k)

Light yellow solid; yield: 85%; mp 141–143 °C; IR (KBr) ν_{\max} 2956, 2908, 1653, 1602, 1508, 1449, 1414, 1231, 1155, 1110, 1048, 922, 834 cm⁻¹; ¹H NMR (DMSO-d₆, 400 MHz) 7.79 (2H, dd, $J = 8.6, 5.6$ Hz, H-2,4), 7.28 (1H, dd, $J = 16.2, 2.7$ Hz, H-8), 7.24 (2H, d, $J = 8.8, 1.6$ Hz, H-3,5), 7.01 (1H, dd, $J = 16.1, 2.2$ Hz, H-7), 6.53 (2H, s, H-3',5'), 5.21 (2H, s, 4'-OCH₂O-), 5.14 (4H, s, 2',6'-OCH₂O-), 3.41 (3H, s, 4'-OCH₃), 3.27 (6H, s, 2',6'-OCH₃); ¹³C NMR (DMSO-d₆, 100 MHz) δ 193.19 (C=O), 163.38 (d, $J = 249.1$ Hz, C-F), 158.87 (C, C-4'), 155.10 (C, C-3',5'), 143.24 (CH, C-8), 130.94 (CH, C-2,6), 130.88 (C, C-1), 128.75 (CH, C-7), 116.11 (CH, C-3), 115.97 (CH, C-5),

114.29 (C, C-1'), 96.59 (CH, C-3',5'), 94.11 (CH₂, 4'-OCH₂O-), 93.99 (CH₂, 2',6'-OCH₂O-), 55.96 (CH₃, 4'-OCH₃), 55.77 (CH₃, 2',6'-OCH₃); EIMS *m/z*: 406.0 [M]⁺.

3,5,7-Trihydroxy-2-phenylchroman-4-one (4a)

White solid; yield: 40%; mp 177–180 °C; IR (KBr) ν_{\max} 3351, 2925, 1640, 1451, 1300, 1042, 820 cm⁻¹; ¹H NMR (DMSO-d₆, 400 MHz): δ = 11.91 (1H, s, OH-5), 10.88 (1H, s, OH-7), 7.53 (2H, d, *J* = 5.7 Hz, H-2',6'), 7.42 (3H, d, *J* = 7.2 Hz, H-3',4',5'), 5.92 (2H, dd, *J* = 16.1, 2.1 Hz, H-6,8), 5.88 (1H, d, *J* = 6.3 Hz, OH-3), 5.19 (1H, d, *J* = 11.4 Hz, H-2), 4.64 (1H, dd, *J* = 11.4, 6.0 Hz, H-3); ¹³C NMR (DMSO-d₆, 100 MHz): δ = 198.0 (C=O, C-4), 167.3 (C, C-7), 163.8 (C, C-5), 162.91 (C, C-9), 137.7 (C, C-1'), 129.1 (CH, C-4'), 128.6 (C, C-3',5'), 128.5 (C, C-2',6'), 100.9 (C, C-10), 96.6 (CH, C-6), 95.5 (CH, C-8), 83.3 (CH, C-2), 71.9 (CH, C-3); EIMS *m/z*: 272.0 [M]⁺.

3,5,7-Trihydroxy-2-(3-hydroxyphenyl)chroman-4-one (4b)

White solid; yield: 55%; mp 201–203 °C; IR (KBr) ν_{\max} 3333, 2913, 1637, 1442, 1280, 1037, 842 cm⁻¹; ¹H NMR (DMSO-d₆, 400 MHz): δ = 12.02 (1H, s, OH-5), 10.91 (1H, s, OH-7), 10.91 (1H, s, OH-3'), 7.14 (1H, t, *J* = 7.4 Hz, H-5'), 7.02 (1H, d, *J* = 7.0 Hz, H-6'), 6.93–6.84 (2H, m, H-2',4'), 5.91 (2H, dd, *J* = 20.8 Hz, 1.4 Hz, H-6,8), 5.72 (1H, d, *J* = 6.2 Hz, OH-3), 5.01 (1H, d, *J* = 11.6 Hz, H-2), 4.48 (1H, dd, *J* = 11.6 Hz, H-3); ¹³C NMR (DMSO-d₆, 100 MHz): δ = 198.1 (C=O, C-4), 168.0 (C, C-7), 164.4 (C, C-5), 163.6 (C, C-9), 158.7 (C, C-3'), 134.9 (CH, C-4'), 130.6 (C, C-1'), 119.9 (CH, C-6'), 116.0 (CH, C-5'), 115.5 (CH, C-2'), 101.2 (C, C-10), 96.7 (CH, C-6), 96.0 (CH, C-8), 83.2 (CH, C-2), 72.6 (CH, C-3); EIMS *m/z*: 288.0 [M]⁺.

3,5,7-Trihydroxy-2-(4-hydroxyphenyl)chroman-4-one (4c)

White solid; yield: 35%; mp 219–220 °C; IR (KBr) ν_{\max} 3327, 2902, 1630, 1462, 1281, 1088, 813 cm⁻¹; ¹H NMR (DMSO-d₆, 400 MHz): δ = 11.92 (1H, s, OH-5), 10.84 (1H, s, OH-7), 9.56 (1H, s, OH-4'), 7.32 (2H, d, *J* = 8.1 Hz, H-2',6'), 6.80 (2H, d, *J* = 8.1 Hz, H-3',5'), 5.90 (2H, d, *J* = 21.4 Hz, H-6,8), 5.76 (1H, d, *J* = 6.1 Hz, OH-3), 5.06 (1H, d, *J* = 11.3 Hz, H-2), 4.59 (1H, dd, *J* = 11.4, 5.6 Hz, H-3); ¹³C NMR (DMSO-d₆, 100 MHz): δ = 198.3 (C=O, C-4), 167.2 (C, C-7), 163.7 (C, C-5), 163.0 (C, C-9), 158.2 (C, C-4'), 129.9 (CH, C-2',6'), 128.0 (C, C-1'), 115.3 (CH, C-3',5'), 100.9 (C, C-10), 96.5 (CH, C-6), 95.4 (CH, C-8), 83.1 (CH, C-2), 71.9 (CH, C-3); EIMS *m/z*: 288.2 [M]⁺.

2-(3,4-Dihydroxyphenyl)-3,5,7-trihydroxychroman-4-one (4d)

White solid; yield: 30%; mp 229–230 °C; IR (KBr) ν_{\max} 3356, 2926, 2854, 1640, 1468, 1283, 1162, 1086, 996, 811, 777, 665 cm⁻¹; ¹H NMR (DMSO-d₆, 400 MHz): δ = 11.89 (1H, s, OH-5), 10.80 (1H, s, OH-7), 9.02 (1H, s, OH-3'), 8.96 (1H, s, OH-4'), 6.85 (1H, s, H-2'), 6.75–6.70 (2H, m, H-5',6'), 5.86 (2H, dd, *J* = 29.2, 2.1 Hz, H-6,8), 5.74 (1H, d, *J* = 6.2 Hz, OH-3), 4.96 (1H, d, *J* = 11.2 Hz, H-2), 4.48 (1H, dd, *J* = 11.2, 6.2 Hz, H-3); ¹³C NMR (DMSO-d₆, 100 MHz): δ = 198.2 (C=O, C-4), 167.2 (C, C-7), 163.7 (C, C-5), 163.0 (C, C-9), 146.2 (C, C-3'), 145.3 (C, C-4'), 128.4 (C, C-1'), 119.8 (CH, C-6'), 115.7 (CH, C-5'), 115.5 (CH, C-2'), 100.9 (C, C-10), 96.4 (CH, C-6), 95.4 (CH, C-8), 83.4 (CH, C-2), 71.9 (CH, C-3); EIMS *m/z*: 305.1 [M]⁺.

3,5,7-Trihydroxy-2-(3,4,5-trihydroxyphenyl)chroman-4-one (4e)

White solid; yield: 25%; mp 234–236 °C; IR (KBr) ν_{\max} 3335, 2911, 1640, 1465, 1288, 1094, 825 cm⁻¹; ¹H NMR (DMSO-d₆, 400 MHz): δ = 12.10 (1H, s, OH-5), 10.89 (1H, s, OH-7), 9.45 (1H, s, OH-4'), 8.89 (1H, s, OH-3'), 8.86 (1H, s, OH-5'), 7.11 (2H, s, H-2',6'), 5.89 (2H, dd, *J* = 9.8, 2.4 Hz, H-6, 8), 5.73 (1H, d, *J* = 6.1 Hz, OH-3), 5.01 (1H, d, *J* = 11.2 Hz, H-2), 4.48 (1H, dd, *J* = 11.2, 6.2 Hz, H-3); ¹³C NMR (DMSO-d₆, 100 MHz): δ = 197.9 (C, C-4), 167.2 (C, C-7), 164.8 (C, C-5), 164.2 (C, C-9), 158.0 (C, C-4'), 145.9 (C, C-3'), 133.8 (C, C-5'), 131.4 (C, C-1'), 116.5 (CH, -2', 6'), 101.5 (C, C-10), 96.7 (CH, C-6), 96.1 (CH, C-8), 81.9 (CH, C-2), 72.4 (CH, C-3); EIMS *m/z*: 320.2 [M]⁺.

3,5,7-Trihydroxy-2-(3-methoxyphenyl)chroman-4-one (4f)

White solid; yield: 37%; mp 134–136 °C; IR (KBr) ν_{\max} 3325, 2918, 1651, 1455, 1286, 1084, 817 cm⁻¹; ¹H NMR (DMSO-d₆, 400 MHz): δ = 11.93 (1H, s, OH-5), 10.98 (1H, s, OH-7), 7.35 (1H, t, *J* = 7.8 Hz, H-5'), 7.12 (2H, d, *J* = 8.0 Hz, H-2',6'), 6.97 (1H, d, *J* = 5.8 Hz, H-4'), 5.96 (2H, d, *J* = 13.1 Hz, H-6,8), 5.88 (1H, s, OH-3), 5.17 (1H, d, *J* = 11.3 Hz, H-2), 4.65 (1H, d, *J* = 11.3 Hz, H-3), 3.79 (3H, s, O-CH₃); ¹³C NMR (DMSO-d₆, 100 MHz): δ = 197.9 (C=O, C-4), 167.3 (C, C-7), 163.8 (C, C-5), 162.8 (C, C-9), 159.6 (C, C-3'), 139.2 (C, C-1'), 129.7 (CH, C-5'), 120.7 (CH, C-6'), 114.4 (CH, C-4'), 114.2 (CH, C-2'), 100.9 (C, C-10), 96.6 (CH, C-6), 95.6 (CH, C-8), 83.3 (CH, C-2), 72.0 (CH, C-3), 55.5 (CH₃, O-CH₃); EIMS *m/z*: 302.0 [M]⁺.

3,5,7-Trihydroxy-2-(4-methoxyphenyl)chroman-4-one (4g)

White solid; yield: 17%; mp 140–142 °C; IR (KBr) ν_{\max} 3327, 2907, 1653, 1463, 1286, 1092, 827 cm^{-1} ; ^1H NMR (DMSO- d_6 , 400 MHz): δ = 11.90 (1H, s, OH-5), 11.01 (1H, s, OH-7), 7.40–7.44 (2H, m, H-2', 6'), 6.92–7.14 (2H, m, H-3', 5'), 6.01 (2H, d, J = 9.6 Hz, H-6, 8), 5.73 (1H, s, OH-3), 4.93 (1H, d, J = 11.2 Hz, H-2), 4.42 (1H, d, J = 11.2 Hz, H-3), 3.80 (3H, s, O-CH₃); ^{13}C NMR (DMSO- d_6 , 100 MHz): δ = 197.9 (C, C-4), 167.2 (C, C-7), 164.0 (C, C-5), 163.4 (C, C-9), 159.5 (C, C-4'), 129.6 (C, C-1'), 128.1 (CH, C-2', 6'), 113.9 (CH, C-3', 5'), 101.2 (C, C-10), 96.7 (CH, C-6), 96.0 (CH, C-8), 84.1 (CH, C-2), 73.1 (CH, C-3), 55.9 (CH₃, O-CH₃); EIMS m/z : 302.2 [M]⁺.

2-(3,4-Dimethoxyphenyl)-3,5,7-trihydroxychroman-4-one (4h)

White solid; yield: 15%; mp 167–170 °C; IR (KBr) ν_{\max} 3333, 2905, 1650, 1460, 1280, 1094, 825 cm^{-1} ; ^1H NMR (DMSO- d_6 , 400 MHz): δ = 11.90 (1H, s, OH-5), 11.01 (1H, s, OH-7), 7.11 (1H, s, H-2'), 6.90–7.02 (2H, m, H-5', 6'), 5.85 (2H, dd, J = 2.1 Hz, H-6, 8), 5.65 (1H, d, J = 6.1 Hz, OH-3), 4.97 (1H, d, J = 11.4 Hz, H-2), 4.49 (1H, dd, J = 11.4 Hz, H-3), 3.89 (3H, s, O-CH₃), 3.86 (3H, s, O-CH₃); ^{13}C NMR (DMSO- d_6 , 100 MHz): δ = 197.6 (C, C-4), 167.2 (C, C-7), 164.2 (C, C-5), 163.4 (C, C-9), 148.6 (C, C-3'), 148.2 (C, C-4'), 129.5 (C, C-1'), 120.5 (CH, C-6'), 111.1 (CH, C-5'), 111.0 (CH, C-2'), 101.2 (C, C-10), 96.7 (CH, C-6), 96.0 (CH, C-8), 83.6 (CH, C-2), 72.4 (CH, C-3), 56.0 (CH₃, O-CH₃); EIMS m/z : 332.3 [M]⁺.

3,5,7-Trihydroxy-2-(4-isopropylphenyl)chroman-4-one (4i)

White solid; yield: 45%; mp 156–157 °C; IR (KBr) ν_{\max} 3320, 2901, 1648, 1462, 1282, 1095, 827 cm^{-1} ; ^1H NMR (DMSO- d_6 , 400 MHz): δ = 11.91 (1H, s, OH-5), 10.86 (1H, s, OH-7), 7.44 (2H, d, J = 8.0 Hz, H-2', 6'), 7.29 (2H, d, J = 7.9 Hz, H-3', 5'), 5.93 (1H, d, J = 2.1 Hz, H-6), 5.88 (1H, d, J = 2.1 Hz, H-8), 5.85 (1H, d, J = 6.3 Hz, OH-3), 5.14 (1H, d, J = 11.4 Hz, H-2), 4.62 (1H, dd, J = 11.4, 6.3 Hz, H-3), 2.92 (1H, hept, J = 7.0 Hz, CH₃-CH-CH₃), 1.23 (6H, s, CH₃-CH-CH₃); ^{13}C NMR (DMSO- d_6 , 100 MHz): δ = 198.1 (C=O, C-4), 167.2 (C, C-7), 163.7 (C, C-5), 162.9 (C, C-9), 149.3 (C, C-4'), 135.2 (C, C-1'), 128.5 (CH, C-2', 6'), 126.6 (CH, C-3', 5'), 100.9 (C, C-10), 96.5 (CH, C-6), 95.5 (CH, C-8), 83.2 (CH, C-2), 73.11 (CH, C-3), 33.7 (CH, CH₃-CH-CH₃), 24.3 (CH₃, CH₃-CH-CH₃); EIMS m/z : 314.1 [M]⁺.

3,5,7-Trihydroxy-2-(4-phenoxyphenyl)chroman-4-one (4j)

White solid; yield: 39%; mp 99–101 °C; IR (KBr) ν_{\max} 3334, 2933, 1651, 1455, 1233, 1088, 838 cm^{-1} ; ^1H NMR

(DMSO- d_6 , 400 MHz): δ = 11.88 (1H, s, OH-5), 10.84 (1H, s, OH-7), 7.10–7.44 (5H, m, OPh-H), 6.88–7.04 (4H, m, H-2', 3', 5', 6'), 5.95 (2H, dd, J = 2.4, H-6, 8), 5.75 (1H, d, J = 6.4 Hz, OH-3), 4.95 (1H, d, J = 11.5 Hz, H-2), 4.43 (1H, dd, J = 11.5 Hz, H-3); ^{13}C NMR (DMSO- d_6 , 100 MHz): δ = 197.9 (C, C-4), 167.2 (C, C-7), 164.29 (C, C-5), 163.53 (C, C-9), 159.50 (C, C-4'), 155.2 (C, OPh-C-1), 129.8 (C, C-1'), 129.1 (CH, OPh-C-3,5), 124.49 (CH, C-2', 6'), 123.9 (CH, OPh-C-4), 120.1 (CH, OPh-C-2,6), 118.69 (CH, C-3', 5'), 101.20 (C, C-10), 96.77 (CH, C-6), 96.05 (CH, C-8), 84.50 (CH, C-2), 72.98 (CH, C-3); EIMS m/z : 364.4 [M]⁺.

2-(4-Fluorophenyl)-3,5,7-trihydroxychroman-4-one (4k)

White solid; yield: 55%; mp 213–215 °C; IR (KBr) ν_{\max} 3337, 2925, 2854, 1639, 1152, 1470, 1230, 1158, 1086, 995, 832, 642 cm^{-1} ; ^1H NMR (DMSO- d_6 , 400 MHz): δ = 11.89 (1H, s, OH-5), 10.88 (1H, s, OH-7), 7.58 (2H, dd, J = 8.6, 5.6 Hz, H-2', 6'), 7.26 (2H, t, J = 8.9 Hz, H-3', 5'), 5.94 (1H, d, J = 2.1 Hz, H-6), 5.89 (1H, d, J = 2.1 Hz, H-8), 5.88 (1H, d, J = 6.2 Hz, OH-3), 5.20 (1H, d, J = 11.5 Hz, H-2), 4.63 (1H, dd, J = 11.6, 6.1 Hz, H-3); ^{13}C NMR (DMSO- d_6 , 100 MHz): δ = 197.6 (C=O, C-4), 166.8 (C, C-7), 163.2 (C, C-5), 162.3 (C, C-9), 161.4 (C, C-4'), 133.6 (C, C-1'), 130.2 (CH, C-2', 6'), 115.1 (CH, C-3', 5'), 100.4 (C, C-10), 96.2 (CH, C-6), 95.1 (CH, C-8), 82.0 (CH, C-2), 71.5 (CH, C-3); EIMS m/z : 291.1 [M]⁺.

2-(4-Chlorophenyl)-3,5,7-trihydroxychroman-4-one (4l)

White solid; yield: 57%; mp 189–192 °C; IR (KBr) ν_{\max} 3331, 2930, 1647, 1450, 1230, 1083, 829 cm^{-1} ; ^1H NMR (DMSO- d_6 , 400 MHz): δ = 11.89 (1H, s, OH-5), 10.90 (1H, s, OH-7), 7.57 (2H, d, J = 8.3 Hz, H-2', 6'), 7.50 (2H, d, J = 8.3 Hz, H-3', 5'), 5.97 (1H, s, H-6), 5.93 (1H, s, H-8), 5.91 (1H, s, OH-3), 5.22 (1H, d, J = 11.5 Hz, H-2), 4.61 (1H, d, J = 10.7 Hz, H-3); ^{13}C NMR (DMSO- d_6 , 100 MHz): δ = 197.7 (C=O, C-4), 167.3 (C, C-7), 163.8 (C, C-5), 162.7 (C, C-9), 136.7 (C, C-4'), 133.7 (C-1'), 130.3 (CH, C-2', 6'), 128.6 (CH, C-3', 5'), 100.9 (C-10), 96.7 (CH, C-6), 95.6 (CH, C-8), 82.5 (CH, C-2), 72.0 (CH, C-3); EIMS m/z : 306.7 [M]⁺.

In vitro anti-inflammatory activities**Cell culture**

RAW 264.7 macrophage cells were obtained from Cell Bank of Academy of Sciences in Huazhong University of Science and Technology (China). The macrophage cells were incubated in Dulbecco's modified Eagle's medium (HyClone, USA) supplemented with 10% fetal bovine

serum (Bovine, China), 100 U/ml penicillin, and 100 µg/ml streptomycin. All cells were incubated at 37 °C in a 5% CO₂ atmosphere during the whole experiment.

Cell viability assay

Mouse RAW 264.7 macrophages were used to analyze the toxicity of dihydroflavonol derivatives. About 8×10^4 cells/well were seeded into 96-well plates and treated with vehicle control or various concentrations of samples for 24 h. 20 µL MTT solution (5 mg/ml) was added to each well and incubated at 37 °C in a humidified atmosphere of 5% CO₂ for 4 h. After MTT removal, 150 µL of dimethyl sulfoxide (DMSO) was added to each well and the assay plate was read at a wavelength of 490 nm using a microplate reader. Three independent experiments were conducted and samples were analyzed in triplicates for each experiment.

Cytokines assay

RAW264.7 cells were cultured at 8×10^4 /well in 96-well plates and preincubated for 12 h. Then, cells were stimulated with LPS (1 µg/ml) for 24 h and the tested compounds in 0.1% DMSO were given at 20 µM for another 24 h. TNF-α, IL-1β, and IL-6 levels were quantified by ELISA kit (eBioScience, Inc.) according to the manufacturer's instructions.

In vivo anti-inflammatory activities

All animals were purchased from Hubei Province Academy of Preventive Medicine. The animal studies were approved by the Hubei University of Traditional Chinese Medicine. All animal studies were conducted according to protocols approved by the Animal Ethics Committee of Hubei Province Hospital of Traditional Chinese Medicine. Animals were housed in separate cages at room temperature 25 ± 2 °C, and given free access to rodent chow, water and maintained at a 12 h light/dark cycle.

Xylene induced ear edema

The in vivo anti-inflammatory activity was evaluated using para-xylene-induced mice ear swelling model in Kunming mice (Li et al. 2017). Kunming mice (22–25 g) were divided into the control group and dosage groups ($n = 10$ for each group).

The negative control group was intragastrically administered with 0.5% carboxymethylcellulose sodium solution. The positive control group was intragastrically administered with standard drug aspirin (100 mg/kg) and meloxicam (10 mg/kg). The remaining test groups were intragastrically

administered with compounds **4d**, **4k** at a dose of 100 mg/kg body weight. After consecutive administration for 7 days, ear swelling was induced by smearing 20 µL para-xylene to each side of right ears. After 1 h, the mice were sacrificed. Both ears at the same position were cut down and weighed. Swelling degree and swelling inhibition were calculated according to the following equations:

$$\text{Swelling degree (mg)} = \text{weight of the right ear} - \text{weight of the left ear}$$

$$\text{Swelling inhibition (\%)} = [W_c - W_d/W_c] \times 100$$

Herein, W_d represents the average swelling degree of dosage group and W_c represents the average swelling degree of control group.

Egg-white induced rat paw edema

The anti-inflammatory activity of compounds **4d**, **4k** was further evaluated using egg-white induced paw edema in rats (Chen et al. 2015). Male Sprague–Dawley rats (150–170 g) were divided into five groups ($n = 6$). The negative control group was intragastrically administered with 0.5% carboxymethylcellulose sodium solution. Positive control groups were intragastrically administered with standard drug aspirin (100 mg/kg) and meloxicam (10 mg/kg). The remaining test groups were intragastrically administered with compounds **4d**, **4k** at a dose of 100 mg/kg body weight. Acute paw edema was induced by sub-plantar injection of 0.1 ml freshly prepared egg-white of each rat after 1 h of administering the test samples. Right hind paw volume was measured with the help of digital plethysmometer through time intervals (0, 30, 60, 120, 180, and 240 min) after induction of inflammation. The percent anti-inflammatory activity was calculated according to the formula given below:

$$\text{Anti-inflammatory activity (\%)} = [V_c - V_t/V_c] \times 100$$

Herein, V_t represents the mean increase in paw volume of rats treated with the test sample and V_c represents the mean increase in paw volume of rats in the control group.

Molecular docking study

Protein preparation

The crystal protein structure of COX-2 (PDB:4M11) (Silva et al. 2018) was downloaded from the Protein Data Bank (<http://www.rcsb.org/pdb/>). The Autodock Tools (Morris et al. 2009) graphics interface was employed for manual preparation of the protein by adding non-polar hydrogen, Gasteiger charges and saved as pdbqt format. 4M11 retains only A chain.

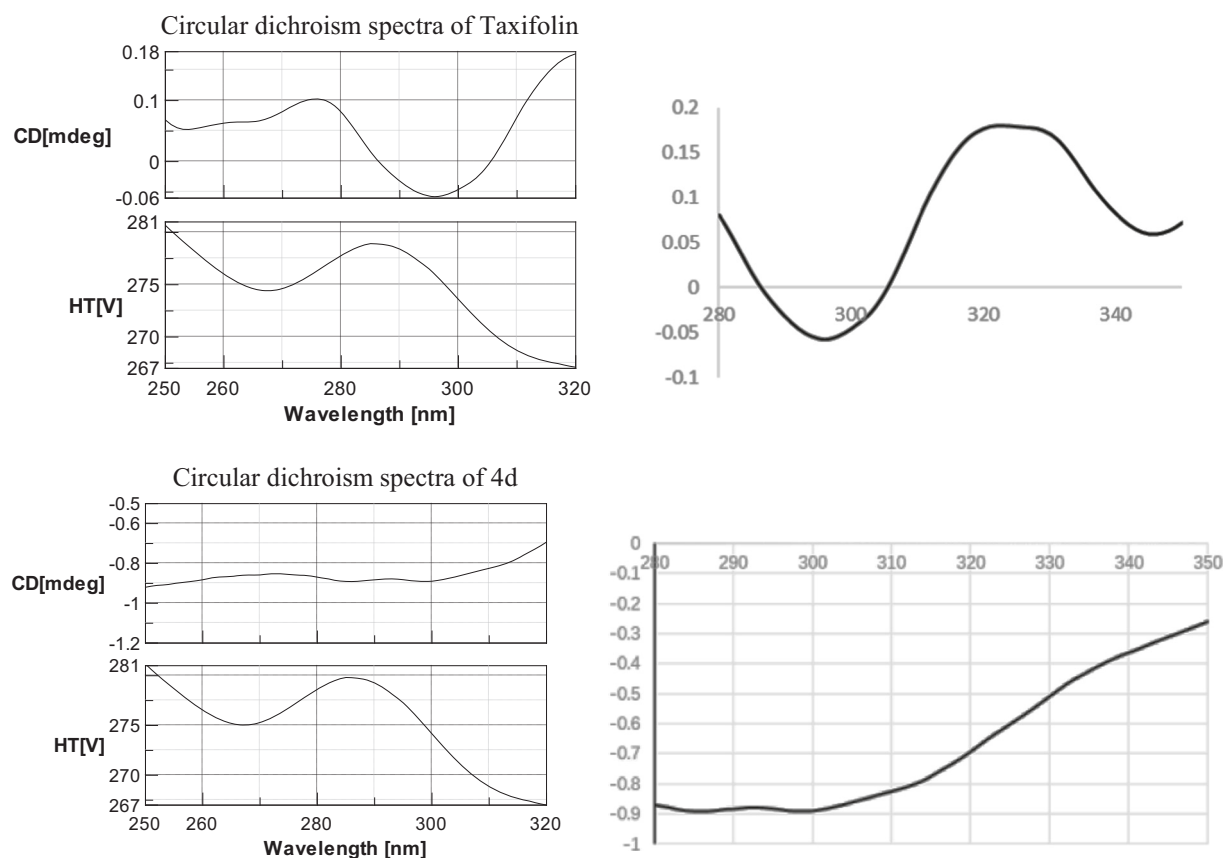


Fig. 1 Circular dichroism spectra of Taxifolin and **4d**

Ligands preparation

Trans isomers were sketched in BIOVIADraw. Openbabel 2.4.1 (O'Boyle et al. 2011) was used to transform 2D into 3D structure by genetic algorithm and MMFF94 force field. Hydrogen was added at pH 7.4 and saved as pdbqt format.

Molecular docking

After the protein and ligand files had been prepared, docking analysis was performed using AutoDock Vina (Trott and Olson 2009). The crystallographic protein structure of COX-2 was selected for docking procedure validation by re-docking approach and also to know the standard docking energy of binding site.

Docking parameters remained the default. Docking output was obtained in the form of affiliate energy (kcal/mol) and binding pose file for each ligand–protein binding conformation. The selected pose was visualized in Pymol v2.1 (Schrödinger 2015). The interaction data were graphically analyzed by Lig-Plus v1.4.5 (Laskowski and Swindells 2011).

Result and discussion

The synthesis of dihydroflavonol derivatives

Synthesis of the intermediates and the target compounds (**4a–4l**) were accomplished according to the steps depicted in Scheme 1. Protection of 2,4,6-trihydroxy acetophenone was achieved with MOMCl to give compound **2**. Then chalcone derivatives (**3a–3l**) were produced by condensation reaction of compounds **2** and corresponding benzaldehydes. Finally, the target compounds (**4a–4l**) were obtained through Algar–Flynn–Oyamada (AFO) reaction by H₂O₂ and hydrochloric acid.

In order to obtain the configuration of synthetic dihydroflavonols, compound **4d** was selected to determine the configuration by proton nuclear magnetic resonance (¹H-NMR) and circular dichroism (CD). By ¹H-NMR analysis of **4d**, the coupling constant of 11.2 Hz between 2H and 3H indicated that **4d** was trans configuration. By CD analysis of **4d**, there was only negative cotton effect at 290–330 nm (Fig. 1). However, there was not only a negative cotton effect at 290–300 nm, but also a positive cotton effect at 320–330 nm for natural Taxifolin (2R,3R), which had the

same chemical structure as **4d**. Above results indicated that the synthetic compound **4d** was racemic mixture. Since it is very difficult to separate these isomers (Jiang et al. 2015) and there was no significant difference in the anti-inflammatory activity between the natural product (Taxifolin) and synthetic product (**4d**) (Hu et al. 2018), we used racemates to further study their anti-inflammatory activities in this paper. All target compounds were characterized by IR, $^1\text{H-NMR}$, $^{13}\text{C-NMR}$, and mass spectroscopy.

In vitro anti-inflammatory activity

Cell viability

To investigate the effect of dihydroflavonol derivatives on RAW 264.7 cell viability, the cells were treated with different concentrations of derivatives (320, 160, 80, 40, 20, 10, and 5 μM) with 1 $\mu\text{g/ml}$ LPS for 24 h. As the results shown in Fig. 2, no cytotoxicity was found after treatment with dihydroflavonol derivatives (**4a–4l**) and Taxifolin at 5, 10, 15, 20, 40 $\mu\text{M/ml}$ for 24 h compared to control group, which demonstrated that cell viability was not significantly affected by up to 20 $\mu\text{M/ml}$ (Fig. 2). Thus, concentrations of 20 $\mu\text{M/ml}$ could be used for follow-up tests.

Inhibition of pro-inflammatory cytokines in RAW 264.7 cell lines

All compounds were evaluated for their in vitro IL-1 β , IL-6, TNF- α inhibition level in LPS induced RAW 264.7 cell lines by ELISA method. Meloxicam was used as positive control. All compounds were screened for their in vitro anti-inflammatory activity, of which **4d**, **4k** showed desirable suppression of IL-1 β , IL-6, TNF- α compared to Meloxicam as the results shown in Fig. 3. According to the result, we chose **4k** and **4d** for further in vivo anti-inflammatory studies.

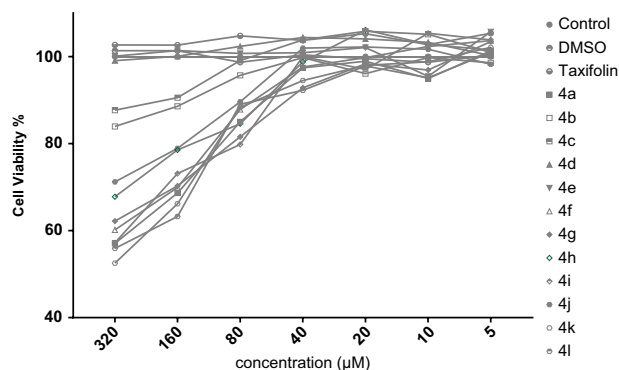


Fig. 2 Cell viability of **4a–4l**

In vivo anti-inflammatory activity

In order to investigate the in vivo anti-inflammatory efficacy of compounds **4d**, **4k**, two different models were employed: xylene induced ear edema in mice and egg-white induced paw edema in rats.

Xylene induced ear-swelling

Ear swelling induced by xylene in mice was used to evaluate the anti-inflammatory activity of compounds **4d**, **4k**. In xylene induced ear edema test, mediators of inflammation are released after following stimulation. This leads to the dilation of arterioles and venules and to increase vascular permeability. As shown in Table 1, the topical application of xylene on the right ear of the control group produced an increase in the average of the ear weight. The administration of **4k** significantly suppressed the ear edema at 32.98% inhibition when compared to the control group ($P < 0.001$), which was nearly the same compared to the 31.99% inhibition delivered by Meloxicam. However, **4d** did not exhibit a considerable anti-inflammatory potential in this model.

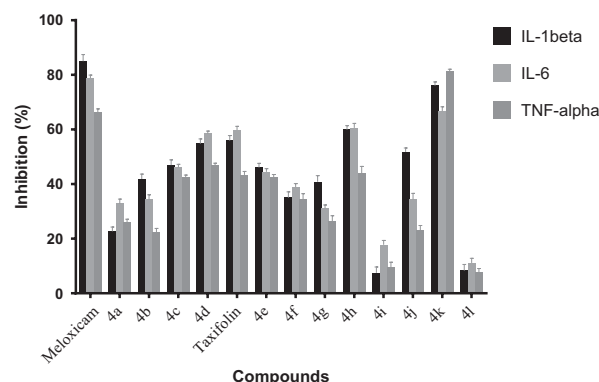


Fig. 3 In vitro IL-1 β , IL-6, TNF- α inhibition of all compounds

Table 1 Anti-inflammatory effect of **4d** and **4k** on xylene induced ear edema in mice

Compound	Dose (mg/kg)	Swelling degree (mg) ^a	Inhibition (%)
Control	–	10.18 \pm 0.53	–
Aspirin	100	5.93 \pm 0.24***	41.73
Meloxicam	10	6.93 \pm 0.61***	31.99
4d	100	8.91 \pm 0.50	12.52
4k	100	6.82 \pm 0.29***	32.98

^aThe results were expressed as mean \pm SEM ($n = 10$), one-way ANOVA test was performed

*** $P < 0.001$ was compared with control

Table 2 The anti-inflammatory activity of **4d**, **4k**, and reference drugs in egg-white induced rat paw edema assay

Compound	Dose (mg/kg)	Mean paw volume (ml) \pm SEM and (% of inhibition) ^a				
		0.5 h	1 h	2 h	3 h	4 h
Control	–	1.052 \pm 0.062	1.180 \pm 0.035	1.165 \pm 0.055	0.992 \pm 0.050	0.842 \pm 0.049
Aspirin	100	1.058 \pm 0.081 (0.00)	1.058 \pm 0.116 (10.31)	0.807 \pm 0.037 (30.76)**	0.602 \pm 0.068 (39.33)***	0.483 \pm 0.068 (42.57)**
Meloxicam	20	1.008 \pm 0.054 (4.12)	1.022 \pm 0.072 (13.42)	0.832 \pm 0.136 (28.61)**	0.695 \pm 0.110 (29.92)*	0.605 \pm 0.092 (28.12)
4d	100	0.983 \pm 0.078 (6.50)	0.933 \pm 0.053 (20.90)*	0.850 \pm 0.065 (27.04)**	0.740 \pm 0.117 (25.38)*	0.515 \pm 0.022 (38.81)**
4k	100	0.855 \pm 0.063 (18.70)	0.718 \pm 0.077 (39.12)***	0.698 \pm 0.092 (40.06)***	0.585 \pm 0.086 (41.01)***	0.553 \pm 0.049 (34.26)*
4k	75	0.815 \pm 0.084 (22.50)	0.855 \pm 0.136 (27.54)**	0.760 \pm 0.113 (34.76)***	0.637 \pm 0.086 (35.80)**	0.532 \pm 0.093 (36.83)**
4k	50	0.908 \pm 0.048 (13.63)	1.073 \pm 0.044 (9.04)	0.795 \pm 0.080 (31.76)**	0.682 \pm 0.076 (31.26)**	0.537 \pm 0.102 (36.24)**

^aOne-way ANOVA using Dunnett's test is applied for statistical analysis. Values are expressed as mean \pm SEM (ml) and percentage inhibition of inflammation

*The mean difference is significant at the $P < 0.05$ level

**The mean difference is significant at the $P < 0.01$ level

***The mean difference is significant at the $P < 0.001$ level

Egg-white induced rat paw edema

The in vivo anti-inflammatory activity of compounds **4d**, **4k** was further evaluated by the egg-white induced paw edema method. As shown in Table 2, the synthesized compounds **4d**, **4k** produced a significant reduction at interval time 1–4 h at 100 mg/kg when compared with the control group. At the interval time 2–4 h, only **4k** showed a higher effect than reference drugs, which indicated that **4k** had the best anti-inflammatory activity. Thus, we further investigated the anti-inflammatory effect of **4k** at lower doses and found the lowest dose of **4k** (50 mg/kg) evidently decreased the percentage inhibition of paw edema at the interval time 2–4 h.

Molecular docking study

In order to gain a better understanding of the potency of the studied compounds, we continued to examine the interaction of the active compound **4k** with COX-2 crystal structure. The molecular docking was performed by inserting the compound **4k** into the binding site of COX-2. Herein, molecules were deeply embedded into the active site pocket and occupy the same position like Meloxicam (shown in yellow color) and the superimposition of Meloxicam and potent **4k** dock poses in the active pocket are shown in Fig. 4.

The molecular basis interactions between target enzyme and synthesized ligands can be understood with the help of docking analysis and interactions. By superposed docking pose of **4k** and meloxicam, almost the same binding mode

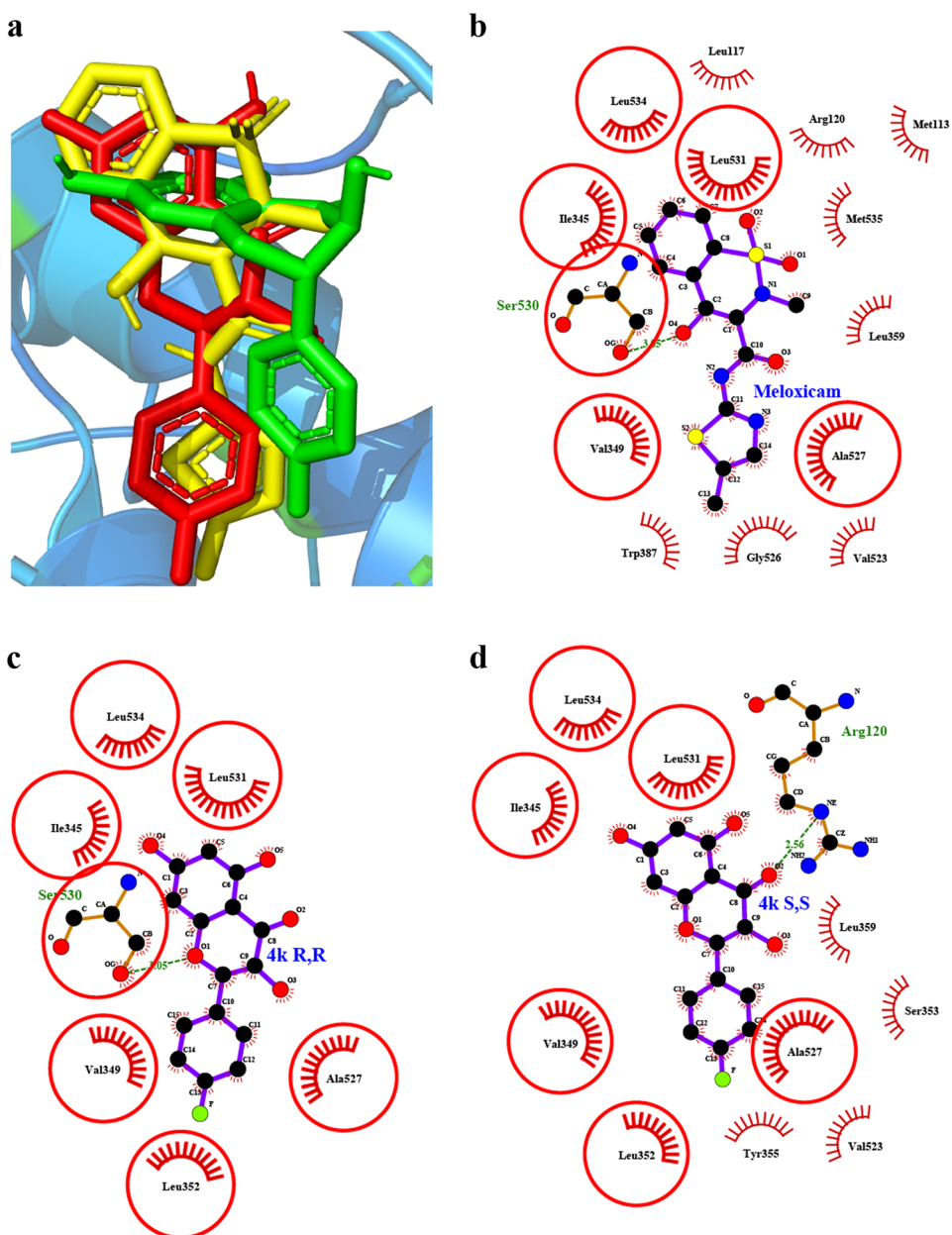
was found (Fig. 4a). Of which, the oxygen atom on the hydroxyl group of Meloxicam and the oxygen atom on the carbonyl group of **4k** (2R,3R isomer) formed two hydrogen bonds with Ser530 at the same distance of 3.05 Å (Fig. 4b, c). However, the oxygen atom on carbonyl group of **4k** (2S,3S isomer) formed a hydrogen bond with Arg120 at the distance of 2.56 Å (Fig. 4d). It was interesting that the F atom of isomers of **4k** (2R,3R and 2S,3S) in the B ring both entered the hydrophobic pocket formed by Val349 and Ala527. Moreover, the binding energy of the 2R,3R isomer (–8.9 kcal/mol) was nearly the same as the 2S,3S isomer (–8.6 kcal/mol). Above results gave a possible mechanistic explanation for the potent activity of **4k**.

Conclusion

We synthesized 12 compounds with 3,5,7-trihydroxy-2-phenylchroman-4-one skeleton by classical AFO reaction and examined their anti-inflammatory activities. All the synthesized compounds are subjected to the evaluation of in vitro TNF-alpha, IL-1beta, IL-6 production inhibition in RAW 264.7 cell lines. Furthermore, the hit compounds **4d**, **4k** were selected to investigate the in vivo anti-inflammatory efficacy by two classical models: xylene induced ear edema and egg-white induced paw edema. Among all, compound **4k** exhibited potent anti-inflammatory activities.

Molecular docking studies also suggested that active compound **4k** interacts with COX-2 enzyme more

Fig. 4 Meloxicam and **4k** docked into the binding site of COX-2. **a** Superposition of meloxicam (yellow) and **4k** (2R,3R in red and 2S,3S in green). **b** Interaction between Meloxicam and COX-2. **c** Interaction between **4k** (2R,3R isomer) and COX-2. **d** Interaction between **4k** (2S,3S isomer) and COX-2



efficiently and is well agreement with anti-inflammatory activity. Therefore, the compound **4k** may be considered as a promising candidate for the development of new anti-inflammatory agent.

Besides, their structure–activity relationships were discussed preliminarily. The results showed that (1) The hydroxyl/methoxy groups substituted in the B ring increases anti-inflammation activity, but two substitutions are better than three substitutions. (2) The introduction of a large sterically hindered group has a slight impact on anti-inflammatory activity. (3) When the 4' position of B-ring

substituted by the fluorine atom, the anti-inflammatory activity of compound (**4k**) was the best.

Acknowledgements The authors would like to extend their sincere appreciation to the National Natural Science Foundation of China for funding this research group (No. 31370378).

Compliance with ethical standards

Conflict of interest The authors declare that they have no conflict of interest.

Publisher's note: Springer Nature remains neutral with regard to jurisdictional claims in published maps and institutional affiliations.

References

- Ayoub IM, Korinek M, Hwang TL, Chen BH, Chang FR, El-Shazly M, Singab ANB (2018) Probing the anti-allergic and anti-inflammatory activity of biflavonoids and dihydroflavonols from *dietes bicolor*. *J Nat Prod* 81:243–253
- Chen CX, Chen JY, Kou JQ, Xu YL, Wang SZ, Zhu Q, Yang L, Qin ZH (2015) Suppression of inflammation and arthritis by orally administrated cardiotoxin from *Naja naja atra*. *Evid-Based Complement Altern Med* 2015:387094
- Cooke JP, Ferrari M (2018) Inflammation-targeted vascular nanomedicine. *Nat Biomed Eng* 2:269–270
- Devi KP, Malar DS, Nabavi SF, Sureda A, Xiao JB, Nabavi SM, Daglia M (2015) Kaempferol and inflammation: from chemistry to medicine. *Pharmacol Res* 99:1–10
- Ding T, Wang SF, Zhang XY, Zai WJ, Fan JJ, Chen W, Bian Q, Luan JY, Shen YL, Zhang YD, Ju DW, Mei XB (2018) Kidney protection effects of dihydroquercetin on diabetic nephropathy through suppressing ROS and NLRP3 inflammasome. *Phytomedicine* 41:45–53
- Hu CL, Zhou ZB, Xiang YH, Song XY, Wang H, Tao KQ, Ye XC (2018) Design, synthesis and anti-inflammatory activity of dihydroflavonol derivatives. *Med Chem Res* 27:194–205
- Jiang WJ, Ishiuchi KI, Furukawa M, Takamiya T, Kitanaka S, Iijima H (2015) Stereospecific inhibition of nitric oxide production in macrophage cells by flavanols: synthesis and the structure–activity relationship. *Bioorg Med Chem* 23:6922–6929
- Karim AM, Nosiba K, El-Rahman FA, Suad A (2016) Antimicrobial dihydroflavonol from Sudanese *Croton zambesicus* Muell. Arg. (Euphorbiaceae) seeds. *Int J Adv Res* 4:1779–1785
- Laskowski RA, Swindells MB (2011) LigPlot+: multiple ligand–protein interaction diagrams for drug discovery. *J Chem Inf Model* 51:2778–2786
- Li J, Li D, Xu Y, Guo Z, Liu X, Yang H, Wu L, Wang L (2017) Design, synthesis, biological evaluation, and molecular docking of chalcone derivatives as anti-inflammatory agents. *Bioorg Med Chem Lett* 27:602–606
- Morris GM, Huey R, Lindstrom W, Sanner MF, Belew RK, Goodsell DS, Olson AJ (2009) AutoDock4 and AutoDockTools4: automated docking with selective receptor flexibility. *J Comput Chem* 30:2785–2791
- Muiva-Mutisya LM, Atilaw Y, Heydenreich M, Koch A, Akala HM, Cheruiyot AC, Brown ML, Irungu B, Okalebo FA, Derese S, Mutai C, Yenesew A (2018) Antiplasmodial prenylated flavanols from *Tephrosia subtriflora*. *Nat Prod Res* 32:1407–1414
- O'Boyle NM, Banck M, James CA, Morley C, Vandermeersch T, Hutchison GR (2011) Open Babel: an open chemical toolbox. *J Cheminform* 3:33
- Silva JC, Oliveira-Júnior RG, Silva MG, Lavor ÉM, Soares JMD, Lima-Saraiva SRG, Diniz TC, Mendes RL, Alencar-Filho EB, Barreiro EJJ, Lima LM, Almeida JRGS (2018) LASSBio-1586, an N-acylhydrazone derivative, attenuates nociceptive behavior and the inflammatory response in mice. *PLoS ONE* 13:e0199009
- Singh M, Kaur M, Silakari O (2014) Flavones: an important scaffold for medicinal chemistry. *Eur J Med Chem* 84:206–239
- Sun X, Chen RC, Yang ZH, Sun GB, Wang M, Ma XJ, Yang LJ, Sun XB (2014) Taxifolin prevents diabetic cardiomyopathy in vivo and in vitro by inhibition of oxidative stress and cell apoptosis. *Food Chem Toxicol* 63:221–232
- Sun Y, Wang C, Meng Q, Liu Z, Huo X, Sun P, Sun H, Ma X, Peng J, Liu K (2018) Targeting P-glycoprotein and SORCIN: dihydromyricetin strengthens anti-proliferative efficiency of adriamycin via MAPK/ERK and Ca²⁺-mediated apoptosis pathways in MCF-7/ADR and K562/ADR. *J Cell Physiol* 233:3066–3079
- Topal F, Nar M, Gocer H, Kalin P, Kocyigit UM, Gulcin I, Alwasel SH (2016) Antioxidant activity of Taxifolin: an activity–structure relationship. *J Enzyme Inhib Med Chem* 31:674–683
- Trott O, Olson AJ (2009) AutoDock Vina: improving the speed and accuracy of docking with a new scoring function, efficient optimization, and multithreading. *J Comput Chem* 31:455–461